



**HAL**  
open science

## Drought affects both photosystems in *Arabidopsis thaliana*

Chen Hu, Eduard Elias, Wojciech Jacek Nawrocki, Roberta Croce

► **To cite this version:**

Chen Hu, Eduard Elias, Wojciech Jacek Nawrocki, Roberta Croce. Drought affects both photosystems in *Arabidopsis thaliana*. *New Phytologist*, 2023, 240 (2), pp.663-675. 10.1111/nph.19171 . hal-04251036

**HAL Id: hal-04251036**

**<https://hal.science/hal-04251036>**

Submitted on 20 Oct 2023

**HAL** is a multi-disciplinary open access archive for the deposit and dissemination of scientific research documents, whether they are published or not. The documents may come from teaching and research institutions in France or abroad, or from public or private research centers.

L'archive ouverte pluridisciplinaire **HAL**, est destinée au dépôt et à la diffusion de documents scientifiques de niveau recherche, publiés ou non, émanant des établissements d'enseignement et de recherche français ou étrangers, des laboratoires publics ou privés.

# Drought affects both photosystems in *Arabidopsis thaliana*

Chen Hu , Eduard Elias , Wojciech J. Nawrocki  and Roberta Croce 

Biophysics of Photosynthesis, Department of Physics and Astronomy and Institute for Lasers, Life and Biophotonics, Faculty of Science, Vrije Universiteit Amsterdam, De Boelelaan 1081, 1081 HV, Amsterdam, the Netherlands

Author for correspondence:  
Roberta Croce  
Email: [r.croce@vu.nl](mailto:r.croce@vu.nl)

Received: 23 April 2023  
Accepted: 14 July 2023

*New Phytologist* (2023)  
doi: 10.1111/nph.19171

**Key words:** *Arabidopsis*, drought, fluorescence, light reactions, photosynthesis, Photosystem I, Photosystem II.

## Summary

- Drought is a major abiotic stress that impairs plant growth and development. Despite this, a comprehensive understanding of drought effects on the photosynthetic apparatus is lacking. In this work, we studied the consequences of 14-d drought treatment on *Arabidopsis thaliana*.
- We used biochemical and spectroscopic methods to examine photosynthetic membrane composition and functionality.
- Drought led to the disassembly of PSII supercomplexes and the degradation of PSII core. The light-harvesting complexes (LHCII) instead remain in the membrane but cannot act as an antenna for active PSII, thus representing a potential source of photodamage. This effect can also be observed during nonphotochemical quenching (NPQ) induction when even short pulses of saturating light can lead to photoinhibition. At a later stage, under severe drought stress, the PSI antenna size is also reduced and the PSI-LHCI supercomplexes disassemble. Surprisingly, although we did not observe changes in the PSI core protein content, the functionality of PSI is severely affected, suggesting the accumulation of nonfunctional PSI complexes.
- We conclude that drought affects both photosystems, although at a different stage, and that the operative quantum efficiency of PSII ( $\Phi_{\text{PSII}}$ ) is very sensitive to drought and can thus be used as a parameter for early detection of drought stress.

## Introduction

Environmental factors such as temperature, salt, and water availability severely affect plants' growth and development. Drought is one of the most severe abiotic stresses limiting crop production world-wide, reducing the average crop yield by > 50% (Daryanto *et al.*, 2016; Fahad *et al.*, 2017; Cohen *et al.*, 2021).

Drought effects on plants are complex and include morphological, physiological, and biochemical responses at the organism and cellular levels. For instance, leaves may lose turgor and become wilted, curled, and yellow (Chaves *et al.*, 2003; Sofo *et al.*, 2005); stomata close, which decreases CO<sub>2</sub> influx and thus limits photosynthesis yield (Medrano *et al.*, 2002); plant growth slows down due to the lower rate of cell division and expansion, which results from an impaired enzymatic activity and lack of energy supply (Farooq *et al.*, 2009). Drought also affects plant development, accelerating the switch from the vegetative to the reproduction phase in an attempt to complete the life cycle (Desclaux & Roumet, 1996).

Drought also affects the activity of essential photosynthetic enzymes, such as Rubisco, leading to a reduced rate of photosynthesis (Reddy *et al.*, 2004). Upon drought stress, the rate of photorespiration increases dramatically, resulting in the production of ROS (Miller *et al.*, 2010; Das & Roychoudhury, 2014) that can damage chlorophyll, protein, DNA, lipids, and other essential macromolecules (Sairam & Tyagi, 2004; Khorobrykh

*et al.*, 2020), ultimately influencing plant metabolism and limiting growth (Flexas & Medrano, 2002; Noctor *et al.*, 2002; Cruz de Carvalho, 2008).

Previous studies indicated that drought induces the reorganization of the thylakoid membrane, specifically affecting the grana stacking, displaying a decrease in the number and layers of grana (Chen *et al.*, 2016; Shao *et al.*, 2016; Pandey *et al.*, 2023). Chlorophyll fluorescence measurements are a noninvasive and rapid method widely used to evaluate the impact of drought stress on Photosystem II (PSII).  $F_v/F_m$ , a parameter used as a proxy of the functionality of PSII, drops upon drought stress (Chen *et al.*, 2016; Yao *et al.*, 2018; Borisova-Mubarakshina *et al.*, 2020), indicating an impaired PSII function. Water oxidation capacity is severely influenced since the oxygen-evolving complex is damaged in drought conditions (Lu & Zhang, 1999; Meng *et al.*, 2016; Gupta, 2020). It was also shown that the major PSII antenna, the light-harvesting complex II (LHCII), detaches from PSII supercomplexes upon short-term drought stress, while the PSII core remains unaffected and only degrades upon long-term drought stress (Giardi *et al.*, 1996; Chen *et al.*, 2009, 2016; Huang *et al.*, 2019). Additionally, the transcript levels of PSII core proteins (e.g. D1, encoded by *PsbA*) and PSII major antenna proteins (i.e. LHCBI and LHCB2) are down-regulated (Hao *et al.*, 1999; Wang *et al.*, 2011; Liu *et al.*, 2019; Borisova-Mubarakshina *et al.*, 2020).

So far, most drought-stress studies have focused on PSII and its antenna, and less attention has been paid to the drought

response of the integrated photosynthetic apparatus and especially of Photosystem I (PSI). In this study, we followed changes in the photosynthetic apparatus of *Arabidopsis thaliana* during 14-d drought treatment, combining biochemical and functional measurements to better understand the effect of drought on the photosynthetic membrane.

## Materials and Methods

### Plants' growth conditions

Wild-type *Arabidopsis thaliana* (L.) Heynh., Col-0) plants were grown under 120  $\mu\text{mol photons m}^{-2} \text{s}^{-1}$  (fluorescence lamp, the spectrum is shown in Supporting Information Fig. S1), 12 h : 12 h, day : night cycle, at 23°C : 19°C, and watered once a week, for 4–5 wk, after which the plants were separated into Water group (grown for additional 14 d with water), Semi-drought group (7-d drought-treated), and Drought group (14-d drought-treated). The plants were grown with soil in pots laid in a tray, and the day the bottom of the tray was dry was considered the first day of drought.

### Relative water content

The fresh weight of leaves was measured immediately after cutting them from the plants. The turgid weight was measured after soaking the (same) leaves in darkness overnight and drying the surface. The dry weight was measured after covering the leaves with aluminum foil and setting them in an oven at 60°C for 5 d (Weatherley, 1980). The relative water content (RWC) was then calculated as:

$$\text{RWC}(\%) = \frac{\text{Fresh weight} - \text{dry weight}}{\text{Turgid weight} - \text{dry weight}}$$

### Thylakoid isolation

*Arabidopsis* leaves were harvested and kept on ice. Thylakoids were isolated under a dim light as described previously (Xu *et al.*, 2015). The isolated thylakoids were resuspended in a buffer containing 20 mM HEPES, pH 7.5, 0.4 M sorbitol, 15 mM NaCl, and 5 mM  $\text{MgCl}_2$ .

### Pigment analysis and leaf chlorophyll content measurements

The absorption spectra of the pigment extracts (in 80% acetone) were recorded with a UV–Vis spectrophotometer (Cary 4000, Agilent, Santa Clara, CA, USA). The chlorophyll *a* : chlorophyll *b* ratio (Chl*a* : Chl*b*) and the chlorophyll : carotenoid ratio (Chl : Car) were obtained by fitting the spectra of the pigment extracts with those of the isolated pigments in 80% acetone as described in Croce *et al.* (2002). The chlorophyll content was calculated using the extinction coefficients from (Porra *et al.*, 1989) and normalized to the leaf dry weight. The relative carotenoid content was obtained by high-performance liquid chromatography (HPLC) analysis according to Croce *et al.* (2002).

### PAM measurements of chlorophyll fluorescence and P700 redox state

$F_V/F_M$  and nonphotochemical quenching (NPQ) kinetics were measured with a Dual-PAM-100 MODULAR fluorimeter (Walz, Germany). The measuring light (red) was set to 3  $\mu\text{mol photons m}^{-2} \text{s}^{-1}$ , the actinic light to 1024 or 71  $\mu\text{mol photons m}^{-2} \text{s}^{-1}$ , and saturating pulses to 4000  $\mu\text{mol photons m}^{-2} \text{s}^{-1}$  (150 ms-long).

Light response curves of the PSI efficiency ( $\Phi_{\text{PSI}}$ ), PSII efficiency ( $\Phi_{\text{PSII}}$ ), and NPQ were measured with a ChlF unit and P700 dual-wavelength (830/875 nm) unit, as described previously (Klughammer & Schreiber, 1994). Y(ND) and Y(NA) represent the quantum yield of nonphotochemical energy dissipation due to PSI donor and acceptor side limitations, respectively. To reach a steady-state, plants were kept for 10 min in darkness or under actinic light before each measurement. The light intensities used are as follows: 14, 38, 71, 127, 217, 340, 532, 826, 1288, and 1955  $\mu\text{mol photons m}^{-2} \text{s}^{-1}$ .

### Blue native gels and 2D SDS

Blue native gel electrophoresis (BN-PAGE) was performed according to Jarvi *et al.* (2011) and Bielczynski *et al.* (2016). The resolving gels were made with an acrylamide gradient from 4% to 12.5% (w/v) T, 3% C (w/w). Here, T is the total concentration of acrylamide and bisacrylamide monomers, and C is the relative concentration of the cross-linker bisacrylamide to the total monomer concentration of acrylamide and bisacrylamide. The stacking gels were made with 4% (w/v) T and 3% C (w/w). Before loading, thylakoids (8  $\mu\text{g}$  of chlorophyll content) were solubilized with 1%  $\alpha$ -DM for 10 min (*n*-Dodecyl- $\alpha$ -D-maltopyranoside; Anatrace, Maumee, OH, US).

The blue native gels' strips were cut and loaded onto a Laemmli-SDS-PAGE for the second dimension (Laemmli, 1970). The stacking and resolving gels were made with 6% T (w/v) and 13% T (w/v), respectively. After electrophoresis, the gels were stained with staining solution (0.1% Coomassie Blue R250 in 10% acetic acid, 40% methanol, and 50%  $\text{H}_2\text{O}$ ) for 2 h and de-stained with de-staining solution (10% acetic acid, 40% methanol, and 50%  $\text{H}_2\text{O}$ ) for 2 h for three times. The proteins were identified based on previous works (Suorsa *et al.*, 2015; Rantala *et al.*, 2017; Nicol *et al.*, 2019).

### Clear native (CN) gels and bands absorption measurement

The CN gels were prepared according to Jarvi *et al.* (2011). A gradient from 4% to 12.5% (w/v) T, 3% C (w/w) was used for the resolving gel, while the stacking gel was composed of 4% (w/v) T and 3% C (w/w). Eight micrograms (chlorophyll) of thylakoids were solubilized with 1%  $\alpha$ -DM for 10 min before loading on the gel. The cathode buffer contained 0.02%  $\alpha$ -DM and 0.05% sodium deoxycholate (DOC).

Room-temperature absorption spectra of the bands of the CN gel were recorded with a BeamBio spectrophotometer, as described in Hu *et al.* (2023).

## Isolation of PSI complexes

The experiments were performed as described previously (Caffarri *et al.*, 2009). The sucrose density gradients (SDG) were built by thawing a frozen tube containing a sucrose solution (0.5 M sucrose, 20 mM Hepes pH 7.5, 0.06%  $\alpha$ -DM) at 4°C. Each tube was loaded with samples of 350  $\mu$ g Chl after solubilization with 1%  $\alpha$ -DM. The gradients were centrifuged for 16 h at 4°C at 160 000 g. The bands were collected with a syringe.

## Immunoblotting

Immunoblottings were performed according to Fristedt *et al.* (2018). Thylakoids were loaded based on the chlorophyll content onto a commercially precast gel (4–12% T (w/v) Bis–Tris Plus; Invitrogen). All the primary antibodies, PsaA (AS06172), PsbC (AS111787), LHCA1 (AS01005), LHCb1 (AS01004), and PSBS (AS09533), were purchased from Agrisera, Vännäs, Sweden. Chemiluminescence was collected by a LAS 4000 Image Analyzer and analyzed with the IMAGEJ software.

## Electro-elution of protein complexes

Electro-elution of protein complexes from the blue native gel was performed as described in previous studies (Koochak *et al.*, 2019; Hu *et al.*, 2023). The band was excised, and the proteins were eluted with a Model 422 Electro-Eluter (Bio-Rad).

## Low-temperature steady-state fluorescence spectroscopy

Low-temperature steady-state fluorescence emission spectra were measured with a Fluorolog spectrophotometer. The sample (OD of 0.05 per cm at  $Q_y$  maximum) was placed in a glass Pasteur pipette inside a transparent Dewar filled with liquid nitrogen. The emission spectra were obtained by exciting the sample at 440 nm and recorded with a 1 nm step range from 600 nm to 800 nm.

## Electrochromic shift measurements

The functional ratio between PSI and PSII reaction centers (RCs) and the antenna size of each photosystem were determined by the electrochromic shift signal (ECS) using a JTS-10 spectrophotometer as described previously (Baillieux *et al.*, 2010). The PSI:PSII ratio was measured with a single turnover flash (630 nm, 5 ns full width at half maximum (FWHM)) based on the ECS signals detected at 520 and 546 nm (white detecting LEDs filtered with 10 nm FWHM Schott filters) before and after infiltration of the leaves with PSII inhibitors. PSII inhibitors (which retain PSI activity) were required to separate the contributions of PSI and PSII. To inhibit PSII, leaves were infiltrated with 200  $\mu$ M 3-(3,4-dichlorophenyl)-1,1-dimethylurea (DCMU), 1 mM hydroxylamine, 10 mM HEPES, and 150 mM sorbitol at pH 7. The  $F_V/F_M$  after inhibitor infiltration was always verified to drop below 0.05, ensuring the inhibition was complete.

The maximal photochemical rates (i.e. antenna size) of PSI and PSII were measured under continuous light (630 nm, 300  $\mu$ mol photons  $m^{-2} s^{-1}$ ). They were calculated from the initial slopes of the ECS time profiles at both 520 and 546 nm before and after PSII inhibition.

## Functional antenna size measurements of PSII by chlorophyll fluorescence induction

Fluorescence induction kinetics were measured with a Dual-PAM 100 MODULAR fluorimeter (Walz, Germany). Leaves were dark-adapted for 20 min and infiltrated with DCMU solution (200  $\mu$ M DCMU, 10 mM HEPES, and 150 mM sorbitol at pH 7). Forty-six  $\mu$ mol photons  $m^{-2} s^{-1}$  light was used for chlorophyll fluorescence induction (250 ms), and then 1952  $\mu$ mol photons  $m^{-2} s^{-1}$  light (50 ms) was performed to verify the closure of the PSII reaction center.

The reciprocal of the integrated area above the DCMU fluorescence curve was used to calculate the PSII antenna size (Lazar & Pospisil, 1999; Tian *et al.*, 2019).

## Time-resolved fluorescence measurements with a streak camera

Time-resolved measurements were performed with a streak camera setup. In this setup, the laser system is composed of a mode-locked Ti:Sa oscillator (Coherent Mira, Coherent, Santa Clara, CA, USA) that seeds a regenerative amplifier (Coherent Rega 9050, Coherent). The regenerative amplifier yielded *c.* 70 fs pulses centered at *c.* 800 nm at a frequency of 250 kHz. The output of the regenerative amplifier was directed through an optical parametric amplifier (Coherent OPA 9400, Coherent) to obtain the frequency-doubled excitation pulses, which were centered at 400 nm. The spectral bandwidth of these pulses was restricted to 10 nm FWHM by means of an interference filter. The excitation pulses were focused into a flow cuvette. The excitation spot diameter was *c.* 100  $\mu$ m and the optical path length in the flow cuvette was 1 mm. The flow speed was set at *c.* 2.5  $ml s^{-1}$ , which allowed a complete refreshment of the sample in the excitation spot every *c.* 10 pulses. The emission from the sample was collected at a right angle and focused into a spectrograph (Chromex 250IS, Pan American Freeway NE, Albuquerque, NM, USA; 50 grooves  $mm^{-1}$ ). The output light of the spectrograph was focused onto the input optics of the streak camera (Hamamatsu C5680, Shizuoka, Japan). The streak camera operated in synchroscan mode and was frequency-locked to the oscillator. The streak camera images were background- and shading corrected. The excitation power used was 2.5  $\mu$ W. To verify whether this excitation power was low enough to keep PSII in the open state, a cross-check measurement with the TCSPC was performed (to be described later): A power study was conducted on the same samples using the TCSPC setup and the resulting kinetic traces were analyzed and compared with the data generated with the streak camera. For both the watered and drought-treated thylakoids, the streak camera and TCSPC data yielded very similar results, confirming that the PSII was also open in the streak

camera measurements. For both the watered and drought-treated thylakoids, a smaller window of *c.* 530 ps was used. For the drought-treated thylakoids, an additional measurement using a 1.5 ns window was performed as this sample displayed contributions from longer-lived species.

The time-resolved data from the streak camera were globally analyzed using the GLOTARAN software (Snellenburg *et al.*, 2012). In the global analysis, the fluorescence decay traces are fitted using the following equation:

$$F(t, \lambda) = \sum_{k=1}^n \text{DAS}_k(\lambda) \times \exp\left(-\frac{t}{\tau_k}\right) \otimes \text{IRF}(t)$$

where  $\text{DAS}_k$  is the decay-associated spectrum and  $\tau_k$  is the related decay lifetime. The instrument response function was estimated as a single Gaussian function. The FWHM of the IRF was determined to be *c.* 6 and *c.* 20 ps for the time range 2 and 4 measurements, respectively. For the drought-treated thylakoids, the data collected in the two time windows were fitted simultaneously. The correspondence between the raw data and the fit results from the global analysis are shown in Figs S2–S4.

#### Time-correlated single-photon counting (TCSPC)

TCSPC measurements were performed with a FluoTime 200 from PICOQUANT. The samples were excited at 468 nm (10 MHz repetition rate), and fluorescence was detected at 680 nm at 20°C. The laser power was 0.15  $\mu\text{W}$ , which was low enough to avoid chlorophyll annihilation and keep PSII RCs open. The measurement at 680 nm was performed as first and last to check that no changes occurred in the samples during the measurements. The decay traces were fitted to a sum of exponentials, in which the amplitudes and the time constants were allowed to vary. The exponentials were convoluted with the instrument response function, which was measured via the fluorescence decay at 680 nm of pinacyanol iodide (FWHM of 92 ps) in methanol at room temperature (van Oort *et al.*, 2008). The fitting was performed with the TREA advanced software (Digris *et al.*, 2014). The fitting quality was evaluated by the chi-squared test and by visual inspection of the fitting residuals.

#### Statistical analysis

Statistical analysis was performed using appropriate tests based on the sample size. For each data set with > 10 data points, the Student's *t*-test was used for comparison. Alternatively, a Kruskal–Wallis rank sum test was performed for data sets with 10 or fewer data points. A statistically significant difference was defined as *P*-value lower than 0.05 (*P* < 0.05).

## Results

Plants of *Arabidopsis thaliana* were divided into Water, Semi-drought, and Drought groups. The plants in the Water group were normally watered (once a week, see the Materials and Methods section for details), while the Drought group was subject to water

deficit for 14 d (Fig. 1). For some of the experiments, we also analyzed plants after 7 d of water deficiency (Semi-drought group).

Although from Day 0 to Day 7, the leaves remained green, at Day 7 *Arabidopsis* plants already displayed early stress traits with some bottom leaves turning slightly reddish-purple. From Day 8 to Day 14, the leaves became purple (or, sometimes, yellowish) and lost turgor. Notably, differences between plants were visible when plants were treated with severe stress (Fig. S5). Yellow leaves were excluded from all the following analyses.

#### Relative water content and pigment composition

After 14 d of drought treatment, the relative water content (RWC) decreased from 71% to 15% and the chlorophyll content dropped to 38% of the initial value (Fig. 2a,b). The Chl*a*:Chl*b* ratio also dropped from 3.3 to 2.5 (Fig. 2c), suggesting an increased antenna-to-core stoichiometry and/or a change in PSI:PSII ratio. The Chl:Car ratio was reduced in water-deficient plants compared with watered ones (Fig. 2d), as in other stress conditions (e.g. high light; Bielczynski *et al.*, 2016). The carotenoid composition of the thylakoid was analyzed using HPLC and the results are shown in Fig. S6. After drought treatment, the content of neoxanthin, antheraxanthin, and lutein increased, while the content of  $\beta$ -carotene decreased. Zeaxanthin, which was absent in the Water sample, appeared in the Drought sample, resulting in a higher de-epoxidation state of the xanthophyll cycle pigments.

#### Composition of protein complexes in the thylakoid membrane

Next, we investigated by native gel electrophoresis how drought affects the composition of the thylakoid membranes. The thylakoids from the Drought group were more resistant to detergent solubilization than those from watered plants (Fig. 3a), suggesting changes in lipid composition/packing relative to the chlorophyll content. Note that the Chl*a*:Chl*b* ratio of the supernatant and pellet of the drought sample was identical (*c.* 2.3), indicating an even solubilization of the membrane. In the Drought group, a reduction in PSII supercomplexes and an increase in free LHClI trimer was observed, indicating a disassembly/higher instability of PSII supercomplexes, in agreement with previous results (Chen *et al.*, 2016). The amount of PSI-LHClI supercomplexes was also lower and a new band with the protein composition (Fig. 3b) and the spectrum (Fig. 3c,d) of the PSI core was detected. Together with the presence of LHClAs in the monomeric band, which was confirmed by immunoblot (Fig. S7), these results suggest that water deficit leads to a partial disassociation of PSI-LHClI (Fig. 3a,b).

The data of the native gels were confirmed by the separation of the individual complexes by sucrose density gradient. In both Water and Drought samples, band 6 contained the PSI-LHClI supercomplex, as indicated by the analysis of the protein composition (Fig. S8b) and the 77 K fluorescence emission spectra (Fig. S8c). However, this band was far less intense in the Drought

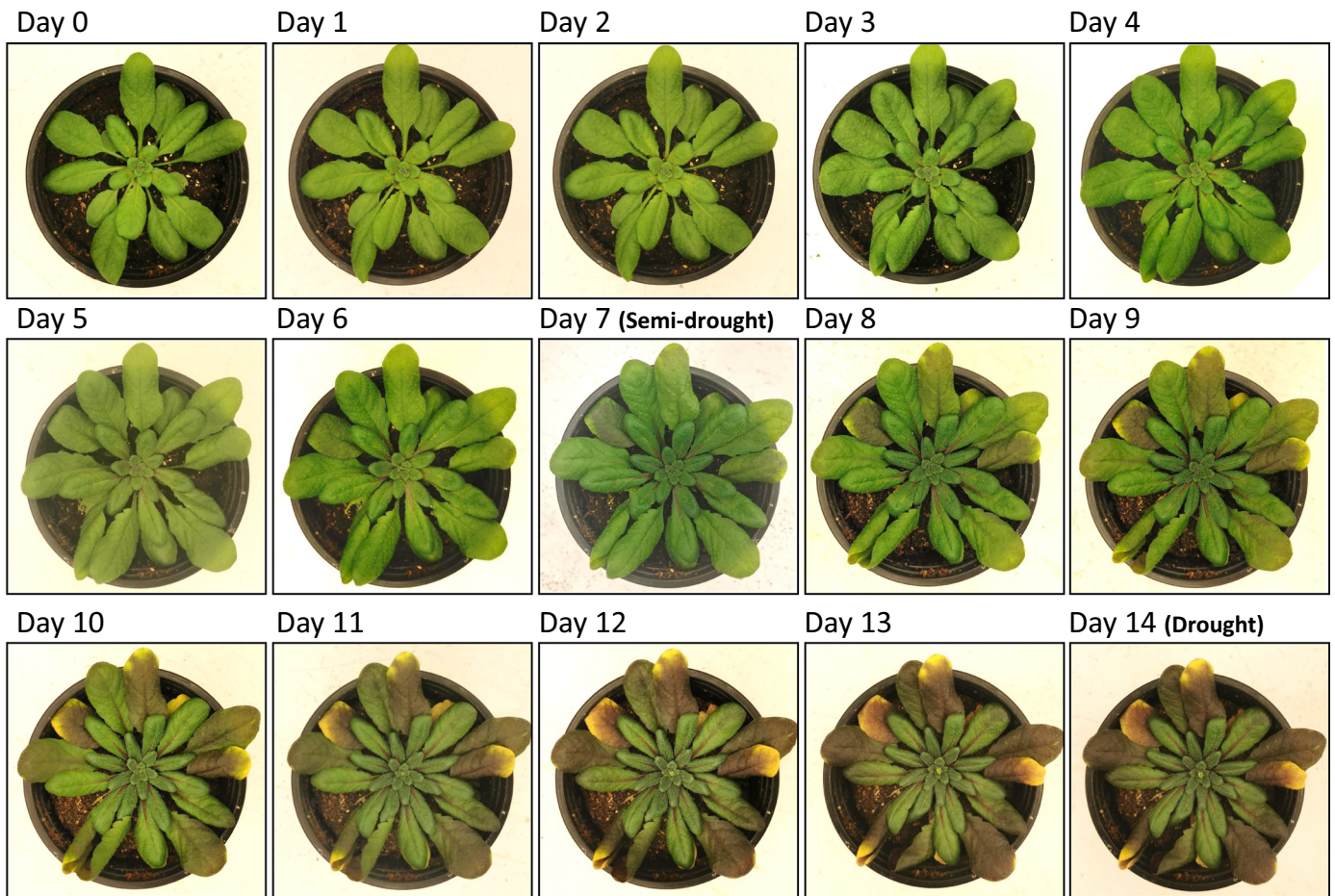
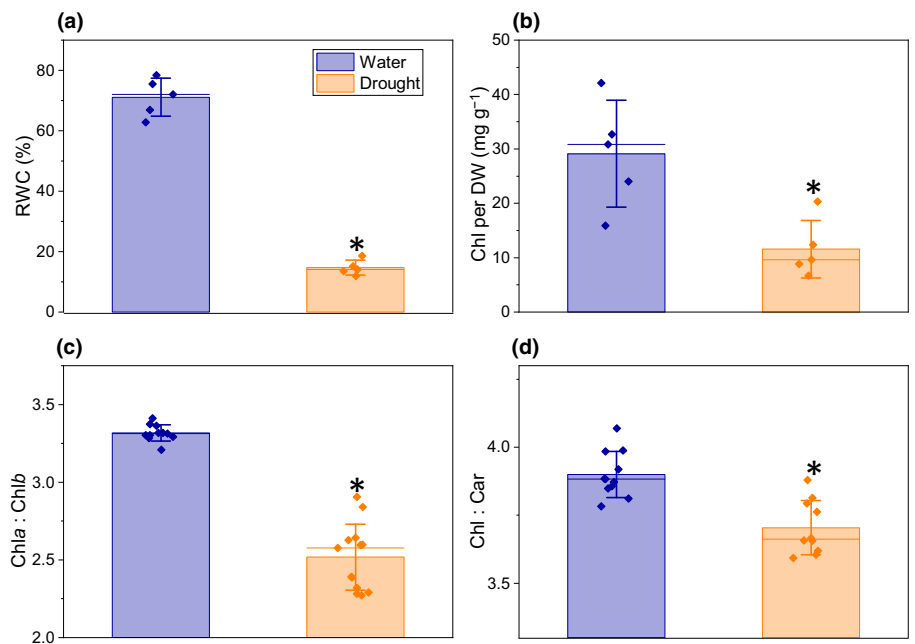


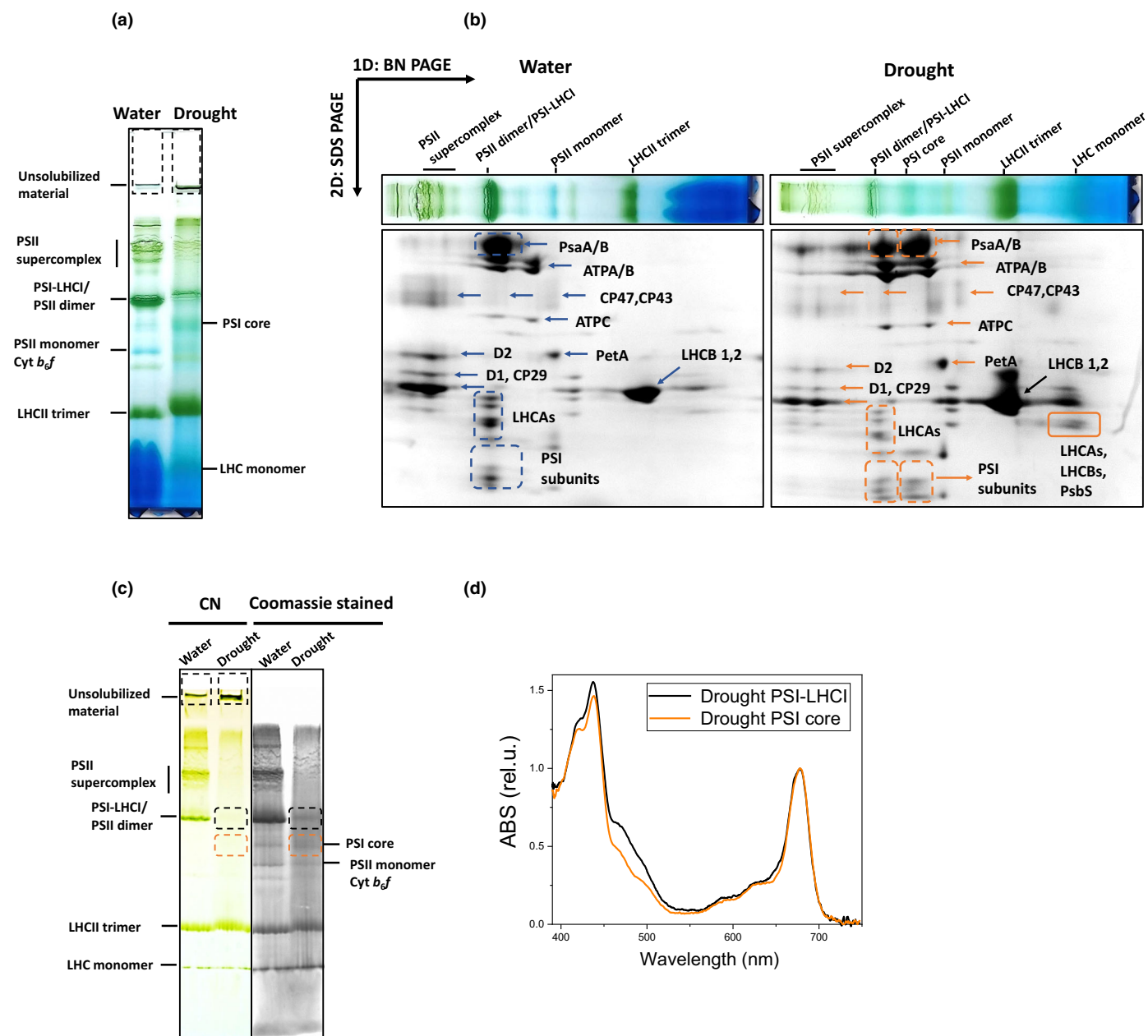
Fig. 1 *Arabidopsis thaliana* plants during the 14-d drought treatment. The images are from the same representative plant.

Fig. 2 Water content and pigment composition of *Arabidopsis* plants watered (blue bars) or drought-treated (orange bars). (a) Relative water content (RWC) and (b) chlorophyll content per dry weight (Chl/DW) of the leaves. (c) Chla : Chlb ratio and (d) Chl : Car ratio of the isolated thylakoids. The asterisks ‘\*’ designate data from the Drought group that are significantly different from those of the corresponding Water group ( $P < 0.05$ , Kruskal–Wallis rank sum test). The bar height represents the mean value; the whiskers stand for  $\pm$ SD ( $n \geq 5$ , independent biological replicates); the additional horizontal line in each bar is the median value. Each individual data point is shown.



sample (Fig. S8a). Band 5 was instead more intense after drought and contained mainly a smaller PSI complex in which the relative amount of all Lhcas, and especially of Lhca3 and

Lhca4 (Fig. S8d) was strongly reduced with respect to the PSI-LHCI complex. In the Water sample, this band was instead enriched in PSII (Fig. S8b,c) as observed previously (Caffarri



**Fig. 3** Analysis of the thylakoid membranes composition from watered and drought-treated Arabidopsis plants. (a) Blue native gels of thylakoids solubilized with 1%  $\alpha$ -DM. Each lane was loaded with 8  $\mu$ g of Chl. (b) Second dimension SDS-PAGE of the blue native gels. The protein composition in the solid square was analyzed using immunoblotting, as illustrated in Supporting Information Fig. S7. (c) Clear native gels of thylakoids solubilized with 1%  $\alpha$ -DM. Each lane was loaded with 8  $\mu$ g of Chl. On the right, the Coomassie blue-stained gel is shown. PSI-LHCI and PSI core bands of Drought Arabidopsis are squared in black and orange, respectively. The room-temperature absorption spectra of the bands, normalized by the Qy maximum, are shown in (d).

*et al.*, 2009). In agreement with the partial loss of LhcAs, which contain the chlorophylls responsible for the 730 nm emission of PSI, the maximum of the 77 K emission spectra of band 5 of the Drought sample was 720 nm (Fig. S8c). Note that the difference in the intensity of band 1 is due to the larger amount of 'free' carotenoids present in the membranes of the drought sample.

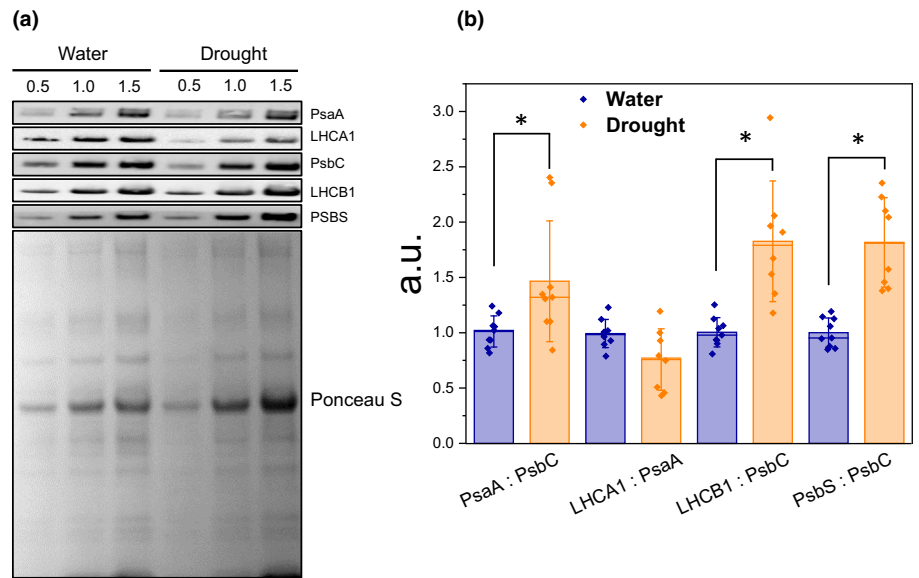
To examine the changes in protein accumulation, we quantified each protein relative to the PSII core subunit PsbC or the PSI core subunit PsaA using immunoblots (Fig. 4). After drought treatment, the PSI:PSII ratio (PsaA:PsbC) increased. The

LHCA1 : PsaA ratio decreased on average but showed large variations between replicas. The LHCb1 : PsbC ratio increased by > 80%, in agreement with the changes observed in *Chl a* : *Chl b* ratios and blue native gels (as mentioned in the previous section). The same increase was observed for the PSBS : PsbC ratio.

#### Functional photosynthetic measurements

Next, we investigated the effect of water deficiency on the functionality of the photosynthetic apparatus. Since plants were

**Fig. 4** Immunoblot analysis of thylakoid proteins from watered and drought-treated Arabidopsis plants. (a) Representative immunoblot images of the target proteins. The antibodies used are indicated on the right side of the blots. The ponceau-stained transferred membrane is also shown. (b) Quantification of photosynthetic proteins. The data were normalized to the respective signal in Water Arabidopsis. The asterisks ‘\*’ designate data from the Drought group that are significantly different from those of the corresponding Water group ( $P < 0.05$ ,  $n = 3$  independent biological replicates, Kruskal–Wallis rank sum test). The bars display mean values  $\pm$ SD. The additional horizontal lines represent median values. Each individual data point is shown.



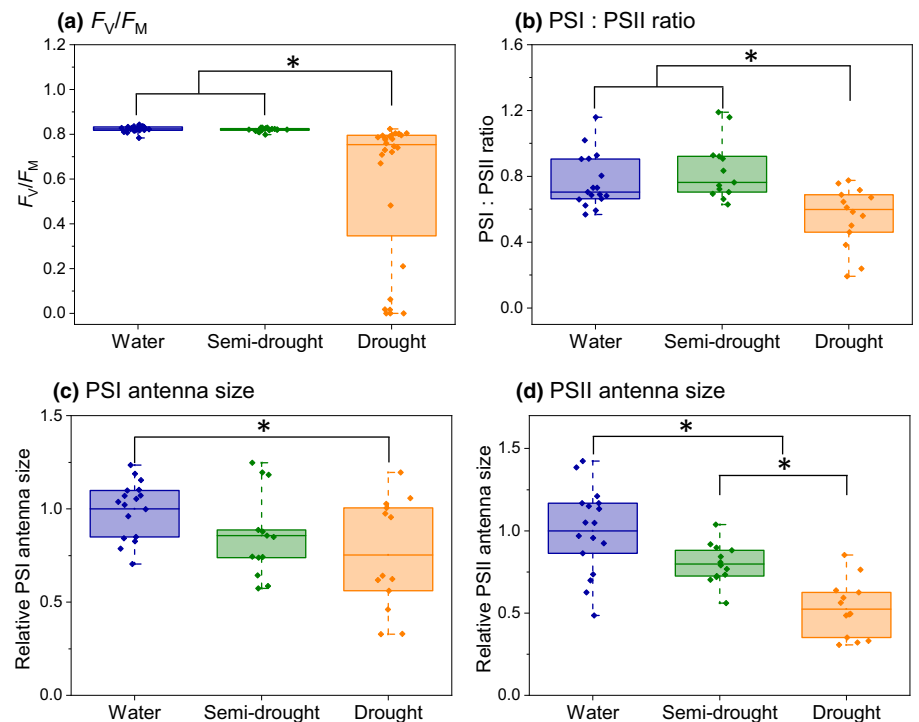
severely affected after 14 d of drought treatment, we also analyzed plants after 7-d (semi-drought) treatment.  $F_V/F_M$ , a proxy for the PSII efficiency, of the semi-drought group was comparable to that of watered plants, whereas the values after 14-d of drought treatment showed a bimodal distribution (Fig. 5a): the reduction was small for a large part of the plants, while others showed almost no PSII activity.

The functional PSI : PSII reaction center (RC) ratio, measured using the electrochromic (ECS) signal, was comparable in the Semi-drought and Water groups and significantly lower in the Drought group (Fig. 5b). This result is in contrast with the increased PsaA : PsbC ratio determined by immunoblots

(Fig. 4b) and might suggest concomitant PSI photoinhibition in drought-stressed plants. The average PSI functional antenna size decreased during drought treatment (Fig. 5c), in agreement with the disassembling of the PSI-LHCI complex observed on blue native gel (Fig. 3). Notably, a large heterogeneity in PSI antenna size was observed upon drought treatment, as some plants still had a PSI antenna size similar to that of the Water group.

Using functional methods, we found no evidence of an increase in PSII antenna size during drought treatment. ECS measurements indicated that the functional antenna size of PSII decreased (Fig. 5d), while no significant differences were observed using the chlorophyll induction method in the presence

**Fig. 5** Functional analysis of the photosynthetic apparatus in watered, semi-drought, or drought-treated Arabidopsis plants. (a)  $F_V/F_M$  value. ECS measurements of (b) PSI : PSII ratio, (c) relative PSI antenna size, and (d) relative PSII antenna size. The antenna size was normalized on the Water group data. Each individual data point is shown ( $n \geq 15$ , independent biological replicates). The asterisks ‘\*’ designate data that are significantly different between the groups ( $P < 0.05$ , Student’s  $t$ -test). The lines in the middle of the boxes represent median values; box borders stand for the first and third quartile; whiskers stand for minimum and maximum. ‘\*’ indicates that the mean difference (MD) between the two groups is statistically significant ( $P < 0.05$ ,  $t$ -test).



of DCMU (Fig. S9). These results are seemingly at odds with the biochemical data, which showed a higher LHCII:PSII core (Lhcb1:Psbc) ratio upon drought. These data together however suggest that part of the LHCII pool in the membrane is not functionally connected to the photochemical traps.

Next, we checked the light intensity dependence of the main photosynthetic parameters. The operating efficiency of Photosystem II ( $\Phi_{PSII}$ ) was lower in the Drought group than in the Water group at all light intensities (Figs 6a, S10). Notably, the results indicate that drought influences the PSII light use efficiency already under mild stress (Semi-drought group, Fig. 6a right).

The NPQ induction kinetics was also measured at a saturating intensity of  $1000 \mu\text{mol photons m}^{-2} \text{s}^{-1}$  (Fig. 6c). Water plants showed the typical NPQ kinetics, with a fast rise reaching a plateau within a few minutes and a relatively fast relaxation in the dark. The Drought group showed a lower NPQ amplitude, which did not reach a plateau in the light, and recovered slower than in the Water group, indicating photoinhibition endured during the measurement. The Semi-drought group showed an intermediate NPQ level (Fig. 6b), but the recovery in the dark was the fastest (Fig. 6c). Surprisingly, the effect of drought

on NPQ was light intensity-dependent: the NPQ values of drought-treated plants were higher than those of the Water group at low light intensities ( $\leq 120 \mu\text{mol photons m}^{-2} \text{s}^{-1}$ ), but lower at higher light intensities (Figs 6c, S10b).

The quantum yield of Photosystem I ( $\Phi_{PSI}$ ) was lower in the Drought group than in the Water group at all light intensities (Figs 6d, S10c). The higher values of  $Y(ND)$  the limitation in PSI donor site, (Figs 6e, S10d) in the Drought group compared with the Water group agree with an impaired PSII function (Figs 5, 6). The comparable low values of  $Y(NA)$  show that the limitation downstream of PSI is not the key factor influencing steady-state electron transfer.

### Time-resolved fluorescence measurements

To investigate the effect of the observed changes in the photosynthetic membrane composition and organization on the excitation energy transfer and trapping of the photosystems, we performed time-resolved fluorescence (TRF) measurements on thylakoids isolated from the Drought and the Water groups. The spectral-temporal images from the streak camera measurements are

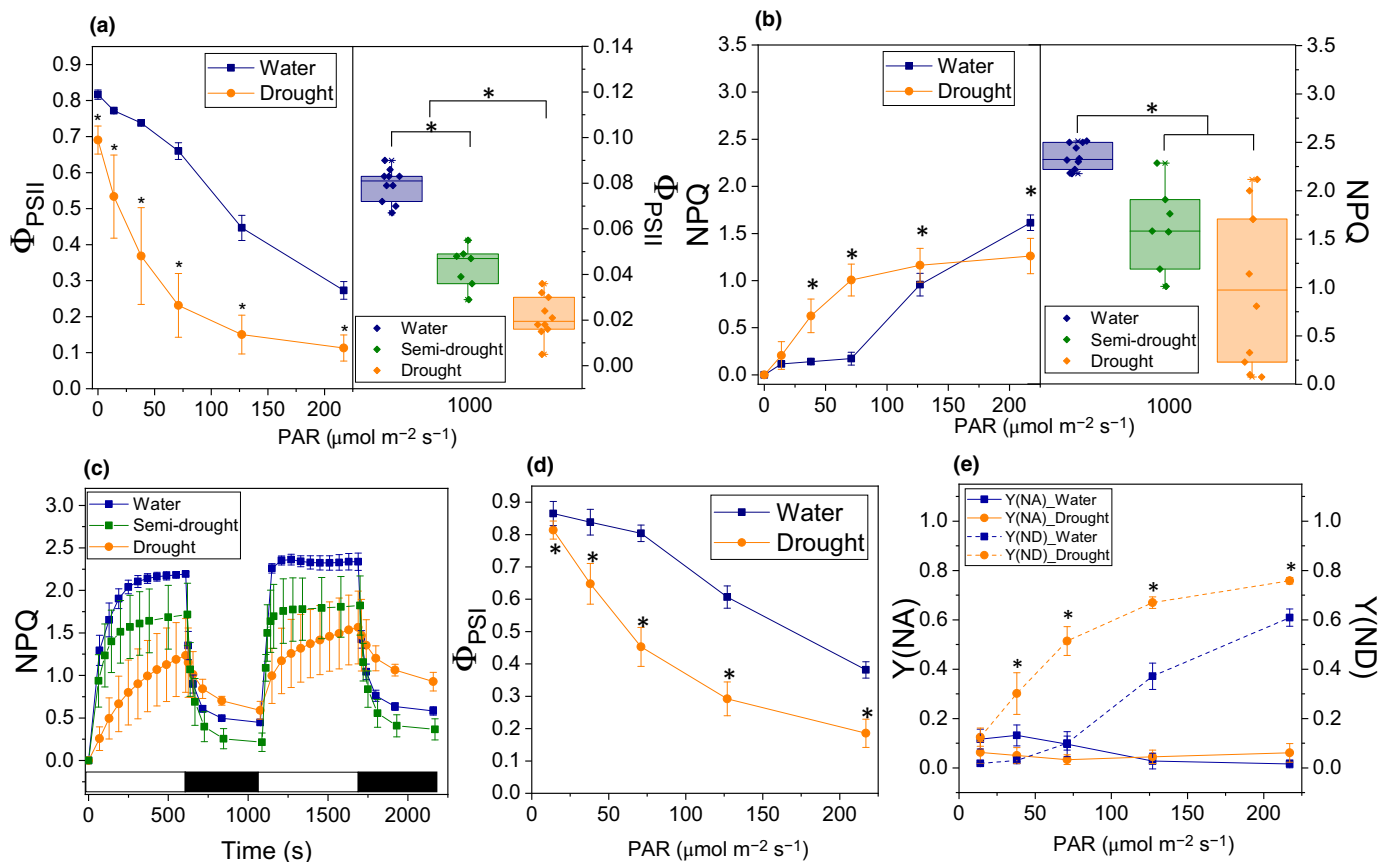


**Fig. 6** Functional measurement of Arabidopsis plants. Light response curves of (a)  $\Phi_{PSII}$  and (b) NPQ at low actinic light ( $0\text{--}220 \mu\text{mol photons m}^{-2} \text{s}^{-1}$ , left) and  $1000 \mu\text{mol photons m}^{-2} \text{s}^{-1}$  (right). (c) NPQ induction and relaxation kinetics (at  $1000 \mu\text{mol photons m}^{-2} \text{s}^{-1}$ ). (d) Quantum yield of PSI ( $\Phi_{PSI}$ ) at different actinic light intensities ( $0\text{--}220 \mu\text{mol photons m}^{-2} \text{s}^{-1}$ ). (e) Donor side limitation ( $Y(ND)$ , solid lines) and acceptor site limitation of PSI ( $Y(NA)$ , dashed lines). All data are average  $\pm$  SD ( $n > 5$ , independent biological samples, Student's  $t$ -test). The gray and black bars below the NPQ kinetics curve (c) represent light and dark periods, respectively. The asterisks '\*' designate data between the groups that are significantly different from each other ( $P < 0.05$ ).

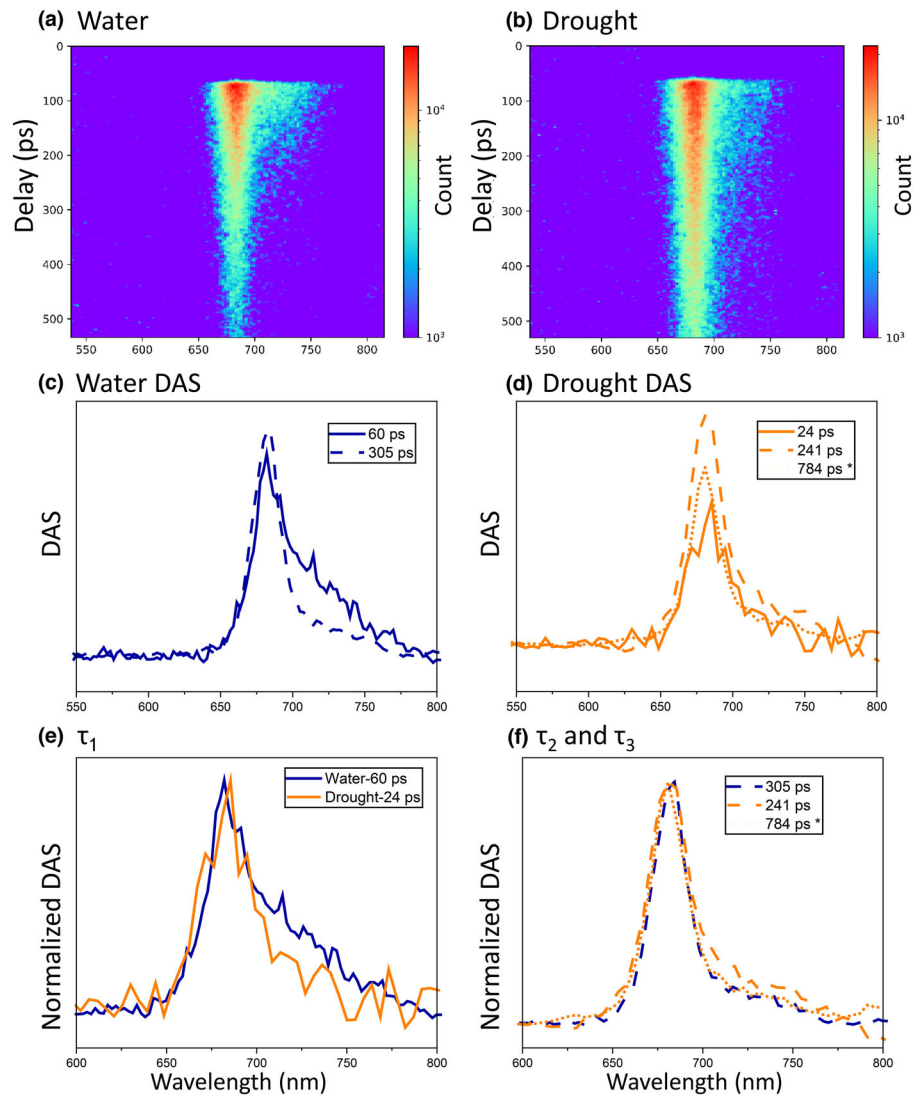


**Fig. 7** Time-resolved fluorescence measurements with open PSII RCs of thylakoids isolated from the water and the drought groups. Data (2D color map) of thylakoid isolated from (a) Water group and (b) Drought group excited at 400 nm. Decay-associated spectra (DAS) of the data of (c) Water and (d) Drought thylakoids. (e) Comparison of the normalized (Nor. In the legend) DAS of the shortest lifetime component from different samples. (f) Comparison of the normalized DAS of the longer components from different samples. The \* indicates that the lifetime of this component was fixed in the analysis (see Supporting Information Notes S1).

presented in Fig. 7(a,b). Comparison of these images already reveals two major points: (1) The fluorescence is longer-lived in the drought thylakoids and (2) there is relatively less emission in the red part of the spectrum ( $\lambda > 700$  nm) at early times in the drought sample. To quantify these observations, global analysis was performed and the resulting DAS are presented in Fig. 7(c,d). Two components are needed to fit the fluorescence kinetics of the Water group (Fig. 7c). The first component has a lifetime of 60 ps and large amplitude in the red part of the spectrum. This component can therefore be assigned to the trapping of excitations by PSI. The second component has lifetime (305 ps) and spectrum typical of PSII. The lifetimes and spectra of both components are comparable to previous studies (Engelmann *et al.*, 2006; van Oort *et al.*, 2010; Wientjes *et al.*, 2011).

Three components are instead needed to fit the data of the Drought group (Fig. 7d). The lifetime of the first component is much shorter (24 ps) than that of the Water group (60 ps, Fig. 7c), and the amplitude in the red part of the spectrum is lower (Fig. 7e). These observations indicate an increased contribution of the PSI core to this component. The second

component has a lifetime of 241 ps and is assigned primarily to PSII, although it also contains some minor contributions of PSI-LHCI, as evidenced by the slightly larger amplitude in the far-red compared with the PSII component of the Water group (Fig. 7f). The shortening of the lifetime of this component relative to the Water thylakoids (241 ps vs 305 ps) indicates a reduced antenna size of PSII, in agreement with the functional analyses (see Fig. 5d). The third component, with a lifetime of 784 ps (see Fig. 7f), displays a spectrum similar to that of the 241 ps component (Fig. 7f) and has a large contribution to the decay (34%, determined from the DAS area). We assign this component to disconnected or poorly connected LHCII trimers, which are also visible in the blue native gel (Fig. 3).

Shortening of the lifetime and loss of amplitude in the far-red of the PSI component upon drought stress suggest a partial disassembly of PSI-LHCI in agreement with the biochemical results. To investigate the properties of the PSI complexes upon drought, we then performed time-resolved measurements on the gradient bands containing PSI complexes (i.e. bands 5 and 6) and compared them to the PSI-LHCI purified from the Water group

(band 6). The results of the global analysis are presented in Fig. S11. Band 6 of the Water sample shows spectra and lifetimes typical of PSI-LHCI (Engelmann *et al.*, 2006; Wientjes *et al.*, 2011): a fast component (4 ps) describing the transfer from bulk Chls *a* to red forms and two trapping components with lifetimes of 19.9 and 81.0 ps, the latter showing higher amplitude in the far-red. These components correspond respectively to trapping from bulk Chls, which are mainly in the core, and red Chls, which are mainly in the LHCI antenna (Wientjes *et al.*, 2011). An additional component with a long lifetime (3.94 ns), small amplitude (5% of the decay components), and a blue-shifted emission peak accounts for a small amount of disconnected Chls in the sample. In Band 6 from the Drought group (Fig. S11b), both trapping components are shorter (16.2 ps and 65.9) and their spectra less red-shifted than in PSI-LHCII. Moreover, the shortest component dominates the decay, at variance with PSI-LHCI from the Water group (see Fig. S11d,e). The additional component of 239 ps has the spectrum and the lifetime of PSII, in agreement with the presence of this complex in this fraction, as visible on the SDS-page (Fig. S8b). Finally, the last component has a long lifetime of 3.46 ns, which is attributed to disconnected Chls.

The decay of band 5 from the drought thylakoids is dominated by the 15.6 ps decay of the PSI core. A second trapping component of PSI is also present, but it has a shorter lifetime than in band 6 (40.6 ps vs 65.9 ps), a smaller amplitude, and the spectrum is less red-shifted (Fig. S11c). This is in agreement with the presence in band 5 of smaller PSI-LHCI, which lack two of the Lhcas as observed in SDS-page (see Fig. S8d,e). The last two decay components (206 ps and 3.52 ns) could be ascribed to a mixture of PSII and free Chls.

## Discussion

### 14-d drought treatment severely impairs photosynthetic activity in Arabidopsis

Drought stress has detrimental effects on plant growth and development. At the level of the photosynthetic apparatus, it was shown that PSII is its primary target (Giardi *et al.*, 1996; Chen *et al.*, 2009; He *et al.*, 2021; Sapeta *et al.*, 2023). In agreement with those results, we found that the PSII activity was reduced and the PSII supercomplexes largely disassembled after 14-d drought treatment. However, while the PSII core was degraded, LHCII was still present in the thylakoid membrane. Considering the high connectivity of the complexes in the membrane (Stirbet, 2013), these LHCII trimers can in principle act as an antenna for the active PSII complexes. However, our functional measurements show that this is not the case: the antenna size of PSII decreased upon drought treatment and a long component appeared in the time-resolved data, indicating that a large pool of LHCII present in the membrane is not connected (and/or not well connected) with the core and is in a partially quenched state. This LHCII pool is also not connected to PSI as a decrease in the antenna size is observed for this complex. The degradation of the LHCII occurs at a slower rate than that of all other

components of the photosynthetic apparatus, posing a threat to the plants through the generation of radical oxygen species that can lead to photodamage.

A decrease in PSII : PSI ratio as a result of drought stress was observed previously in wheat (*Triticum aestivum* L.) and Arabidopsis and was proposed to be functional to an increase in cyclic electron flow around PSI, optimizing the ATP : NADPH ratio for the metabolic needs (Zivcak *et al.*, 2013; Chen *et al.*, 2016; Nawrocki *et al.*, 2019). Moreover, it was reported that PSI was stable upon water deficiency (Havaux *et al.*, 1986; Masojidek *et al.*, 1991; Giardi *et al.*, 1996; Sonoike, 2011; Chen *et al.*, 2016). Our data show that while a decrease in PSII : PSI ratio is observed at the protein level, surprisingly, this does not correspond to a decrease at the functional level. On the contrary, we observed an increase in the functional PSII : PSI ratio, which indicates the presence in the membranes of nonfunctional PSI proteins. However, it should be noted that the variability of the PSI : PSII values upon 14 d of drought treatment is very large, with some plants showing values close to those of the Water group, while in others, the value is strongly reduced. These data suggest that the damage of PSI occurs only upon severe drought stress. A lag between the functional damage of PSI and the protein degradation was also observed in chilled plants (Tjus *et al.*, 1999; Kudoh & Sonoike, 2002; Zhang & Scheller, 2004). A scheme summarizing the effect of drought on PSI and PSII is shown in Fig. 8.

### NPQ and drought stress

The effect of drought stress on NPQ capacity is debated. It was reported that in drought conditions, plants protect themselves from photodamage by increasing NPQ, which rapidly dissipates the excess absorbed energy as heat (Woo *et al.*, 2008; Zivcak *et al.*, 2013). However, other authors reported that drought stress impairs the mechanism of energy dissipation, thus lowering NPQ (Sperdoui & Moustakas, 2012; Yao *et al.*, 2018). Our data reconcile these results: the NPQ values of the Drought group were higher than those of the Water group in low actinic light ( $< 120 \mu\text{mol photons m}^{-2} \text{s}^{-1}$ ) but lower in saturating light (Fig. S11b). Part of this difference is due to the higher susceptibility of the drought-stressed plants to photoinhibition occurring during the NPQ measurements when saturating pulses are used (see Fig. 6c). NPQ induction and recovery kinetics under low actinic light (at  $71 \mu\text{mol photons m}^{-2} \text{s}^{-1}$ , as shown in Fig. S12) show that the Drought group had higher NPQ values than the Water group but exhibit slow dark recovery, indicating that in low light, the NPQ value in the drought group is dominated by photoinhibition. In high light, the NPQ value of the Water group increases because of the large qE induction, while qE induction is limited in the Drought leaves due to the impairment of PSII, which results in a lower luminal pH.

### $\Phi_{\text{PSII}}$ is a good indicator of early drought stress

Drought is one of the most significant abiotic stress factors affecting crop productivity and food security world-wide. Early

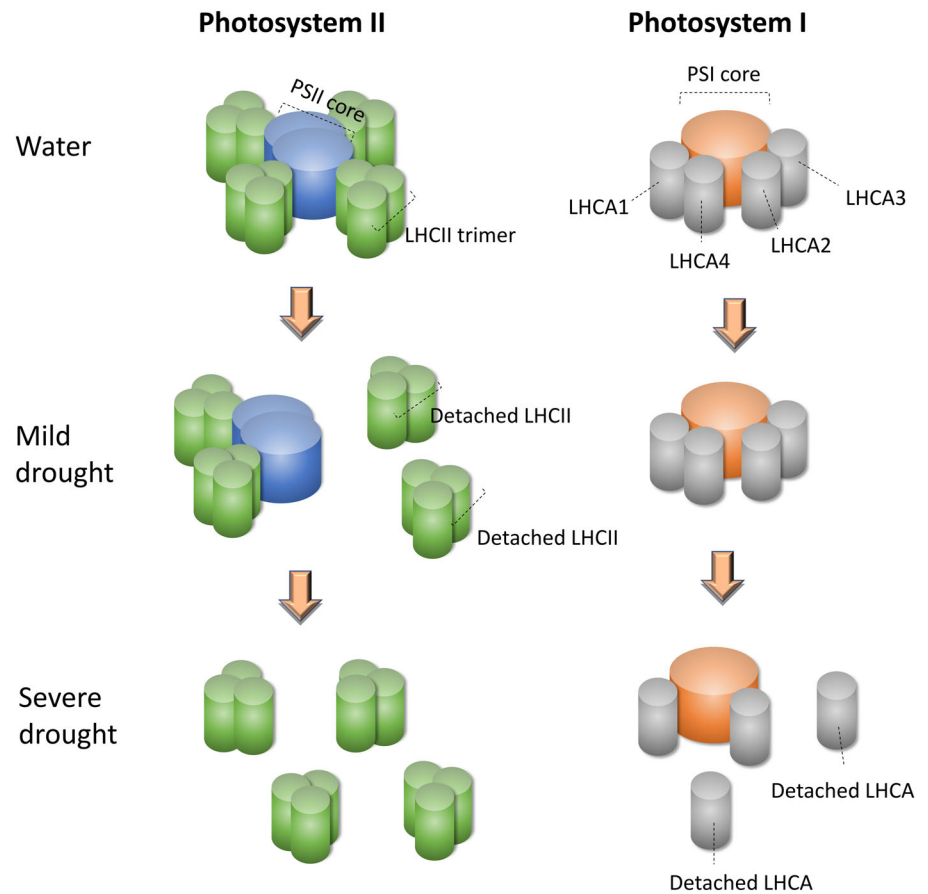


**Fig. 8** Schematic diagram illustrating the impact of drought on the photosystems in *Arabidopsis* plants. Drought affects both photosystems at different stages. LHCII, light-harvesting complex II; LHCA, light-harvesting complexes specific for PSI; PSI, Photosystem I; PSII, Photosystem II.

detection of drought stress is thus important since it allows for prompt actions to mitigate its negative effects.  $F_v/F_M$  is often regarded as a sensitive indicator of drought stress (Oquist *et al.*, 1992; Woo *et al.*, 2008). However, our data show that it only dropped by *c.* 20% after 14 d of water deficiency (Fig. 4a) and showed no change after 7 d of treatment, despite the leaves already exhibited some phenotypic alterations. By contrast, we could observe a decrease in  $\Phi_{PSII}$  already after 7 d, indicating that  $\Phi_{PSII}$  is more sensitive than  $F_v/F_M$  and therefore is a better indicator of early drought stress.

## Acknowledgements

This project was partially supported by the Dutch Organization for scientific research (NWO) via a TOP grant to RC.

## Competing interests

None declared.

## Author contributions

RC and CH conceived and designed the experiments. CH, EE and WJN performed the experiments and the data analysis. RC and CH wrote the paper. All the authors reviewed and edited the manuscript.

## ORCID

Roberta Croce [ID https://orcid.org/0000-0003-3469-834X](https://orcid.org/0000-0003-3469-834X)  
 Eduard Elias [ID https://orcid.org/0000-0002-2048-5629](https://orcid.org/0000-0002-2048-5629)  
 Chen Hu [ID https://orcid.org/0000-0002-0015-1402](https://orcid.org/0000-0002-0015-1402)  
 Wojciech J. Nawrocki [ID https://orcid.org/0000-0001-5124-3000](https://orcid.org/0000-0001-5124-3000)

## Data availability

The data that support the findings of this study are available in the [Supporting Information](#) of this article.

## References

- Bailleul B, Cardol P, Breyton C, Finazzi G. 2010. Electrochromism: a useful probe to study algal photosynthesis. *Photosynthesis Research* 106: 179–189.
- Bielczynski LW, Schansker G, Croce R. 2016. Effect of light acclimation on the organization of Photosystem II super- and sub-complexes in *Arabidopsis thaliana*. *Frontiers in Plant Science* 7: 105.
- Borisova-Mubarakshina MM, Vetoshkina DV, Naydov IA, Rudenko NN, Zhurikova EM, Balashov NV, Ignatova LK, Fedorchuk TP, Ivanov BN. 2020. Regulation of the size of Photosystem II light-harvesting antenna represents a universal mechanism of higher plant acclimation to stress conditions. *Functional Plant Biology* 47: 959–969.
- Caffarri S, Kouril R, Kereiche S, Boekema EJ, Croce R. 2009. Functional architecture of higher plant Photosystem II supercomplexes. *EMBO Journal* 28: 3052–3063.

- Chaves MM, Maroco JP, Pereira JS. 2003. Understanding plant responses to drought – from genes to the whole plant. *Functional Plant Biology* 30: 239–264.
- Chen YE, Liu WJ, Su YQ, Cui JM, Zhang ZW, Yuan M, Zhang HY, Yuan S. 2016. Different response of Photosystem II to short and long-term drought stress in *Arabidopsis thaliana*. *Physiologia Plantarum* 158: 225–235.
- Chen YE, Yuan S, Du JB, Xu MY, Zhang ZW, Lin HH. 2009. Phosphorylation of photosynthetic antenna protein CP29 and Photosystem II structure changes in monocotyledonous plants under environmental stresses. *Biochemistry* 48: 9757–9763.
- Cohen I, Zandalinas SI, Huck C, Fritschi FB, Mittler R. 2021. Meta-analysis of drought and heat stress combination impact on crop yield and yield components. *Physiologia Plantarum* 171: 66–76.
- Croce R, Canino G, Ros F, Bassi R. 2002. Chromophore organization in the higher-plant Photosystem II antenna protein CP26. *Biochemistry* 41: 7334–7343.
- Cruz de Carvalho MH. 2008. Drought stress and reactive oxygen species: production, scavenging and signaling. *Plant Signaling & Behavior* 3: 156–165.
- Daryanto S, Wang L, Jacinthe PA. 2016. Global synthesis of drought effects on maize and wheat production. *PLoS ONE* 11: e0156362.
- Das K, Roychoudhury A. 2014. Reactive oxygen species (ROS) and response of antioxidants as ROS-scavengers during environmental stress in plants. *Frontiers in Environmental Science* 2: 53.
- Desclaux D, Roumet P. 1996. Impact of drought stress on the phenology of two soybean (*Glycine max* L. Merr) cultivars. *Field Crops Research* 46: 61–70.
- Digris AV, Novikov EG, Skakun VV, Apanasovich VV. 2014. Global analysis of time-resolved fluorescence data. In: Engelborghs Y, Visser A, eds. *Fluorescence spectroscopy and microscopy. Methods in molecular biology (methods and protocols)*. Totowa, NJ, USA: Humana Press, 257–277.
- Engelmann E, Zucchelli G, Casazza AP, Brogioli D, Garlaschi FM, Jennings RC. 2006. Influence of the Photosystem I-light harvesting complex I antenna domains on fluorescence decay. *Biochemistry* 45: 6947–6955.
- Fahad S, Bajwa AA, Nazir U, Anjum SA, Farooq A, Zohaib A, Sadia S, Nasim W, Adkins S, Saud S *et al.* 2017. Crop production under drought and heat stress: plant responses and management options. *Frontiers in Plant Science* 8: 1147.
- Farooq M, Basra SMA, Wahid A, Ahmad N, Saleem BA. 2009. Improving the drought tolerance in rice (*Oryza sativa* L.) by exogenous application of salicylic acid. *Journal of Agronomy and Crop Science* 195: 237–246.
- Flexas J, Medrano H. 2002. Energy dissipation in C-3 plants under drought. *Functional Plant Biology* 29: 1209–1215.
- Fristedt R, Hu C, Wheatley N, Roy LM, Wachter RM, Savage L, Harbinson J, Kramer DM, Merchant SS, Yeates T. 2018. RAF 2 is a RuBis CO assembly factor in *Arabidopsis thaliana*. *The Plant Journal* 94: 146–156.
- Giardi M, Cona A, Geiken B, Kučera T, Masojidek J, Mattoo A. 1996. Long-term drought stress induces structural and functional reorganization of Photosystem II. *Planta* 199: 118–125.
- Gupta R. 2020. The oxygen-evolving complex: a super catalyst for life on earth, in response to abiotic stresses. *Plant Signaling & Behavior* 15: 1824721.
- Hao L, Liang H, Wang Z, Liu X. 1999. Effects of water stress and rewetting on turnover and gene expression of Photosystem II reaction center polypeptide D1 in *Zea mays*. *Functional Plant Biology* 26: 375–378.
- Havaux M, Canaan O, Malkin S. 1986. Photosynthetic responses of leaves to water stress, expressed by photoacoustics and related methods: II. The effect of rapid drought on the electron transport and the relative activities of the two photosystems. *Plant Physiology* 82: 834–839.
- He W, Yan K, Zhang Y, Bian L, Mei H, Han G. 2021. Contrasting photosynthesis, photoinhibition and oxidative damage in honeysuckle (*Lonicera japonica* Thunb.) under iso-osmotic salt and drought stresses. *Environmental and Experimental Botany* 182: 104313.
- Hu C, Mascoli V, Elias E, Croce R. 2023. The photosynthetic apparatus of the CAM plant *Tillandsia flabellata* and its response to water deficit. *Journal of Plant Physiology* 282: 153945.
- Huang B, Chen YE, Zhao YQ, Ding CB, Liao JQ, Hu C, Zhou LJ, Zhang ZW, Yuan S, Yuan M. 2019. Exogenous melatonin alleviates oxidative damages and protects Photosystem II in maize seedlings under drought stress. *Frontiers in Plant Science* 10: 677.
- Jarvi S, Suorsa M, Paakkarinen V, Aro EM. 2011. Optimized native gel systems for separation of thylakoid protein complexes: novel super- and mega-complexes. *Biochemical Journal* 439: 207–214.
- Khorobrykh S, Havurinne V, Mattila H, Tyystjarvi E. 2020. Oxygen and ROS in photosynthesis. *Plants* 9: 91.
- Klughammer C, Schreiber U. 1994. An improved method, using saturating light-pulses, for the determination of photosystem-I quantum yield via P700+ absorbency changes at 830 Nm. *Planta* 192: 261–268.
- Koochak H, Puthiyaveetil S, Mullendore DL, Li M, Kirchhoff H. 2019. The structural and functional domains of plant thylakoid membranes. *The Plant Journal* 97: 412–429.
- Kudoh H, Sonoike K. 2002. Irreversible damage to Photosystem I by chilling in the light: cause of the degradation of chlorophyll after returning to normal growth temperature. *Planta* 215: 541–548.
- Laemmli U. 1970. SDS-page Laemmli method. *Nature* 227: 680–685.
- Lazar D, Pospisil P. 1999. Mathematical simulation of chlorophyll a fluorescence rise measured with 3-(3',4'-dichlorophenyl)-1,1-dimethylurea-treated barley leaves at room and high temperatures. *European Biophysics Journal* 28: 468–477.
- Liu J, Guo YY, Bai YW, Li HJ, Xue JQ, Zhang RH. 2019. Response of photosynthesis in maize to drought and re-watering. *Russian Journal of Plant Physiology* 66: 424–432.
- Lu C, Zhang J. 1999. Effects of water stress on Photosystem II photochemistry and its thermostability in wheat plants. *Journal of Experimental Botany* 50: 1199–1206.
- Masojidek J, Trivedi S, Halshaw L, Alexiou A, Hall DO. 1991. The synergistic effect of drought and light stresses in Sorghum and pearl-millet. *Plant Physiology* 96: 198–207.
- Medrano H, Escalona JM, Bota J, Gulias J, Flexas J. 2002. Regulation of photosynthesis of C-3 plants in response to progressive drought: stomatal conductance as a reference parameter. *Annals of Botany* 89: 895–905.
- Meng LL, Song JF, Wen J, Zhang J, Wei JH. 2016. Effects of drought stress on fluorescence characteristics of photosystem II in leaves of *Plectranthus scutellarioides*. *Photosynthetica* 54: 414–421.
- Miller G, Suzuki N, Ciftci-Yilmaz S, Mittler R. 2010. Reactive oxygen species homeostasis and signalling during drought and salinity stresses. *Plant, Cell & Environment* 33: 453–467.
- Nawrocki WJ, Bailleul B, Picot D, Cardol P, Rappaport F, Wollman FA, Joliot P. 2019. The mechanism of cyclic electron flow. *Biochimica et Biophysica Acta (BBA) – Bioenergetics* 1860: 433–438.
- Nicol L, Nawrocki WJ, Croce R. 2019. Disentangling the sites of non-photochemical quenching in vascular plants. *Nature Plants* 5: 1177–1183.
- Noctor G, Veljovic-Jovanovic S, Driscoll S, Novitskaya L, Foyer CH. 2002. Drought and oxidative load in the leaves of C-3 plants: a predominant role for photorespiration? *Annals of Botany* 89: 841–850.
- van Oort B, Alberts M, de Bianchi S, Dall'Osto L, Bassi R, Trinkunas G, Croce R, van Amerongen H. 2010. Effect of antenna-depletion in Photosystem II on excitation energy transfer in *Arabidopsis thaliana*. *Biophysical Journal* 98: 922–931.
- van Oort B, Amunts A, Borst JW, van Hoek A, Nelson N, van Amerongen H, Croce R. 2008. Picosecond fluorescence of intact and dissolved PSI-LHCI crystals. *Biophysical Journal* 95: 5851–5861.
- Oquist G, Chow WS, Anderson JM. 1992. Photoinhibition of photosynthesis represents a mechanism for the long-term regulation of photosystem-II. *Planta* 186: 450–460.
- Pandey J, Devadasu E, Saini D, Dhokne K, Marriboina S, Raghavendra AS, Subramanyam R. 2023. Reversible changes in structure and function of photosynthetic apparatus of pea (*Pisum sativum*) leaves under drought stress. *The Plant Journal* 113: 60–74.
- Porra R, Thompson W, Kriedemann P. 1989. Determination of accurate extinction coefficients and simultaneous equations for assaying chlorophylls a and b extracted with four different solvents: verification of the concentration of chlorophyll standards by atomic absorption spectroscopy. *Biochimica et Biophysica Acta (BBA) – Bioenergetics* 975: 384–394.
- Rantala M, Tikkanen M, Aro EM. 2017. Proteomic characterization of hierarchical megacomplex formation in Arabidopsis thaliana thylakoid membrane. *The Plant Journal* 92: 951–962.

- Reddy AR, Chaitanya KV, Vivekanandan M. 2004. Drought-induced responses of photosynthesis and antioxidant metabolism in higher plants. *Journal of Plant Physiology* 161: 1189–1202.
- Sairam R, Tyagi A. 2004. Physiology and molecular biology of salinity stress tolerance in plants. *Current Science* 1: 407–421.
- Sapeta H, Yokono M, Takabayashi A, Ueno Y, Cordeiro AM, Hara T, Tanaka A, Akimoto S, Oliveira MM, Tanaka R. 2023. Reversible down-regulation of photosystems I and II leads to fast photosynthesis recovery after long-term drought in *Jatropha curcas*. *Journal of Experimental Botany* 74: 336–351.
- Shao RX, Xin LF, Zheng HF, Li LL, Ran WL, Mao J, Yang QH. 2016. Changes in chloroplast ultrastructure in leaves of drought-stressed maize inbred lines. *Photosynthetica* 54: 74–80.
- Snellenburg J, Laptanok S, Seger R, Mullen K, van Stokkum IHM. 2012. GLOTARAN: a Java-based graphical user interface for the R package TIMP. *Journal of Statistical Software* 49: 1–22.
- Sofa A, Tuzio AC, Dichio B, Xiloyannis C. 2005. Influence of water deficit and rewatering on the components of the ascorbate–glutathione cycle in four interspecific *Prunus* hybrids. *Plant Science* 169: 403–412.
- Sonoike K. 2011. Photoinhibition of Photosystem I. *Physiologia Plantarum* 142: 56–64.
- Sperdoui I, Moustakas M. 2012. Differential response of Photosystem II photochemistry in young and mature leaves of *Arabidopsis thaliana* to the onset of drought stress. *Acta Physiologiae Plantarum* 34: 1267–1276.
- Stirbet A. 2013. Excitonic connectivity between Photosystem II units: what is it, and how to measure it? *Photosynthesis Research* 116: 189–214.
- Suorsa M, Rantala M, Mamedov F, Lespinasse M, Trotta A, Grieco M, Vuorio E, Tikkanen M, Jarvi S, Aro EM. 2015. Light acclimation involves dynamic re-organization of the pigment–protein mega-complexes in non-appressed thylakoid domains. *The Plant Journal* 84: 360–373.
- Tian LJ, Nawrocki WJ, Liu X, Polukhina I, van Stokkum IHM, Croce R. 2019. pH dependence, kinetics and light-harvesting regulation of nonphotochemical quenching in *Chlamydomonas*. *Proceedings of the National Academy of Sciences, USA* 116: 8320–8325.
- Tjus SE, Moller BL, Scheller HV. 1999. Photoinhibition of Photosystem I damages both reaction centre proteins PSI-A and PSI-B and acceptor-side located small Photosystem I polypeptides. *Photosynthesis Research* 60: 75.
- Wang YX, Suo B, Zhao TF, Qu XF, Yuan LG, Zhao XJ, Zhao HJ. 2011. Effect of nitric oxide treatment on antioxidant responses and psbA gene expression in two wheat cultivars during grain filling stage under drought stress and rewatering. *Acta Physiologiae Plantarum* 33: 1923–1932.
- Weatherley PE. 1980. Citation classic – studies in the water relations of the cotton plant. 1. The field measurement of water deficits in leaves. *Current Contents/Agriculture Biology & Environmental Sciences* 49: 10.
- Wientjes E, van Stokkum IH, van Amerongen H, Croce R. 2011. The role of the individual Lhcas in Photosystem I excitation energy trapping. *Biophysical Journal* 101: 745–754.
- Woo NS, Badger MR, Pogson BJ. 2008. A rapid, non-invasive procedure for quantitative assessment of drought survival using chlorophyll fluorescence. *Plant Methods* 4: 1–14.
- Xu PQ, Tian LJ, Kloz M, Croce R. 2015. Molecular insights into Zeaxanthin-dependent quenching in higher plants. *Scientific Reports* 5: 1–10.
- Yao J, Sun D, Cen H, Xu H, Weng H, Yuan F, He Y. 2018. Phenotyping of *Arabidopsis* drought stress response using kinetic chlorophyll fluorescence and multicolor fluorescence imaging. *Frontiers in Plant Science* 9: 603.
- Zhang SP, Scheller HV. 2004. Photoinhibition of Photosystem I at chilling temperature and subsequent recovery in *Arabidopsis thaliana*. *Plant and Cell Physiology* 45: 1595–1602.
- Zivcak M, Brestic M, Balatova Z, Drevenakova P, Olsovska K, Kalaji HM, Yang X, Allakhverdiev SI. 2013. Photosynthetic electron transport and specific photoprotective responses in wheat leaves under drought stress. *Photosynthesis Research* 117: 529–546.

## Supporting Information

Additional Supporting Information may be found online in the Supporting Information section at the end of the article.

**Fig. S1** Spectra of the light used for growing the plants.

**Fig. S2** Time-resolved fluorescence streak camera data and fitting of Water sample in the 530 ps time window.

**Fig. S3** Time-resolved fluorescence streak camera data and fitting of Drought sample in the 530 ps time window.

**Fig. S4** Time-resolved fluorescence streak camera data and fitting of Drought sample in the 1.5 ns time window.

**Fig. S5** Variability of the effect of 14-d drought treatment on *Arabidopsis* plants.

**Fig. S6** HPLC analysis on carotenoid composition in thylakoid from Water and Drought-treated plants.

**Fig. S7** Immunoblot analysis of the BN gel band containing Lhc monomers (in solid square in Fig. 3b) of Drought *Arabidopsis*.

**Fig. S8** Isolation of PSI complexes.

**Fig. S9** Functional antenna size of PSII measured with Chl fluorescence induction.

**Fig. S10** Light response curves of photosynthetic parameters:  $\Phi_{\text{PSII}}$ , NPQ,  $\Phi_{\text{PSI}}$ , Y(NA), and Y(ND).

**Fig. S11** Global analysis of TRF of PSI complexes isolated by sucrose density gradient.

**Fig. S12** NPQ induction and relaxation kinetics upon low actinic light (at  $71 \mu\text{mol photons m}^{-2} \text{s}^{-1}$ ).

**Notes S1** Fixed long lifetime component in the global analysis of the streak measurements.

Please note: Wiley is not responsible for the content or functionality of any Supporting Information supplied by the authors. Any queries (other than missing material) should be directed to the *New Phytologist* Central Office.